ALGORITHM THEORETICAL BASIS DOCUMENT (ATBD) - SINGLE ASPIRATED AIR TEMPERATURE

PREPARED BY	ORGANIZATION	DATE
Derek Smith	FIU	01/06/2014
Josh Roberti	FIU	09/28/2015
Robert Clement	FIU	02/10/2010
Jesse Vance	AQU	02/05/2015

APPROVALS	ORGANIZATION	APPROVAL DATE
Andrea Thorpe	SCI	10/23/2015
Dave Tazik	SCI	10/13/2015
Hanne Buur	PSE	10/20/2015

RELEASED BY	ORGANIZATION	RELEASE DATE
Jennifer DeNicholas	CM	10/23/2015

See configuration management system for approval history.

The National Ecological Observatory Network is a project solely funded by the National Science Foundation and managed under cooperative agreement by NEON, Inc. Any opinions, findings, and conclusions or recommendations expressed in this material are those of the author(s) and do not necessarily reflect the views of the National Science Foundation.

Change Record

REVISION	DATE	ECO #	DESCRIPTION OF CHANGE
A	05/14/2013	ECO-00777	Initial Release
B	08/29/2013	ECO-01224	Update with new algorithms
C	10/23/2015	ECO-03110	Updated document to reflect L0 and L1 data product renumbering Revised *Algorithm Implementation* and *Uncertainty* Sections, Added aquatic meteorology station information. Implemented standardized coverage factor of k=2 Moved consistency analyses outline to Future Plans / Modifications Sections

TABLE OF CONTENTS

LIST OF TABLES AND FIGURES

1 DESCRIPTION

Contained in this document are details concerning temperature measurements made at all NEON sites. Specifically, the processes necessary to convert "raw" sensor measurements into meaningful scientific units and their associated uncertainties are described. Temperature will be continuously monitored by NEON at core and relocatable sites by two methods. Temperature for the top of the tower will be derived from the triple redundant aspirated air temperature sensor and will be discussed in additional documents. This document focuses on the Single Aspirated Air Temperature Sensors (SAATS) that will be used to develop temperature profiles and on the micromet station at NEON aquatic sites. Temperature profiles will be ascertained by deploying SAATS at various heights on the core tower infrastructure and mobile platforms. Air temperature at aquatic sites will be measured using a single SAAT at a standard height of 3m above ground level.

1.1 Purpose

This document details the algorithms used for creating NEON Level 1 data products for a single SAATS from Level 0 data, and ancillary data as defined in this document (such as calibration data). It includes a detailed discussion of measurement theory and implementation, appropriate theoretical background, data product provenance, quality assurance and control methods used, approximations and/or assumptions made, and a detailed exposition of uncertainty resulting in a cumulative reported uncertainty for this product.

1.2 Scope

The theoretical background and entire algorithmic process used to derive Level 1 data from Level 0 data for the SAATS are described in this document. The temperature sensor employed is the Thermometrics Climate RTD 100 Ω Probe, which is housed in a Met One 076B fan aspirated radiation shield to reduce error from direct and indirect radiation. This document does not provide computational implementation details, except for cases where these stem directly from algorithmic choices explained here.

2 RELATED DOCUMENTS, ACRONYMS AND VARIABLE NOMENCLATURE

2.1 Applicable Documents

AD[01]	NEON.DOC.000001	NEON OBSERVATORY DESIGN
AD[02]	NEON.DOC.005003	NEON Scientific Data Products Catalog
AD[03]	NEON.DOC.002652	NEON Level 1, Level 2 and level 3 Data Products Catalog
AD[04]	NEON.DOC.005005	NEON Level 0 Data Products Catalog
AD[05]	NEON.DOC.000782	ATBD QA/QC Data Consistency
AD[06]	NEON.DOC.011081	ATBD QA/QC plausibility tests
AD[07]	NEON.DOC.000783	ATBD De-spiking and time series analyses
AD[08]	NEON.DOC.000746	Evaluating Uncertainty (CVAL)
AD[09]	NEON.DOC.000302	C^3 Single Aspirated Air Temperature
AD[10]	NEON.DOC.000723	Triple Point Temperature Calibration Fixture
AD[11]	NEON.DOC.002002	Engineering Master Location Sensor Matrix
AD[12]	NEON.DOC.000784	ATBD Profile Development
AD[13]	NEON.DOC.000785	TIS Level 1 Data Products Uncertainty Budget Estimation Plan
AD[14]	NEON.DOC.000751	CVAL Transfer of standard procedure
AD[15]	NEON.DOC.000927	NEON Calibration and Sensor Uncertainty Values[1]
AD[16]	NEON.DOC.001113	Quality Flags and Quality Metrics for TIS Data Products
AD[17]	NEON.DOC.000780	ATBD 2D Wind Speed and Direction
AD[18]	NEON.DOC.001450	C^3 AQU Single Aspirated Air Temperature

2.2 Reference Documents

RD[01]	NEON.DOC.000008	NEON Acronym List
RD[02]	NEON.DOC.000243	NEON Glossary of Terms

2.3 Acronyms

Acronym	Explanation
AIS	Aquatic Instrument System
ATBD	Algorithm Theoretical Basis Document
CVAL	NEON Calibration, Validation, and Audit Laboratory

[1] Note that CI obtains calibration and sensor values directly from an XML file maintained and updated by CVAL in real time. This report is updated approximately quarterly such that there may be a lag time between the XML and report updates.

DAS	Data Acquisition System
DP	Data Product
FDAS	Field Data Acquisition System
GRAPE	Grouped Remote Analog Peripheral Equipment
L0	Level 0
L1	Level 1
N/A	Not Applicable
NOAA	National Oceanic Atmospheric Administration
PRT	Platinum Resistance Thermometer
RTD	Resistance Temperature Detectors
SAAT	Single Aspirated Air Temperature
SAATS	Single Aspirated Air Temperature Sensor

2.4 Variable Nomenclature

The symbols used to display the various inputs in the ATBD, e.g., calibration coefficients and uncertainty estimates, were chosen so that the equations can be easily interpreted by the reader. However, the symbols provided will not always reflect NEON's internal notation, which is relevant for CI's use, and or the notation that is used to present variables on NEON's data portal. Therefore a lookup table is provided in order to distinguish what symbols specific variables can be tied to in the following document.

Symbol	**Internal Notation**	**Description**
C_0	CVALA0	CVAL PRT calibration coefficient
C_1	CVALA1	CVAL PRT calibration coefficient
C_2	CVALA2	CVAL PRT calibration coefficient
O_R	U_CVALR4	offset imposed by the FDAS for resistance readings (Ω)
u_{A1}	U_CVALA1	Combined, relative uncertainty of PRT sensor (%)
u_{A3}	U_CVALA3	Combined, relative uncertainty (truth and trueness only) of PRT sensor (%)
u_{R1}	U_CVALR1	Combined, relative uncertainty of Field DAS resistance readings (%)
u_{R3}	U_CVALR3	Combined, relative uncertainty (truth and trueness only) of Field DAS resistance readings (%)

2.5 Verb Convention

"Shall" is used whenever a specification expresses a provision that is binding. The verbs "should" and "may" express non-mandatory provisions. "Will" is used to express a declaration of purpose on the part of the design activity.

3 DATA PRODUCT DESCRIPTION

3.1 Variables Reported

The single aspirated air temperature related L1 DPs provided by the algorithms documented in this ATBD are displayed in the accompanying file sat_datapub_NEONDOC002874.txt.

3.2 Input Dependencies

Table 3-1 details the SAATS-related L0 DPs used to produce L1 SAAT DPs in this ATBD.

Table 3-1 List of SAATS-related L0 DPs that are transformed into L1 SAAT DPs in this ATBD.

Description	Sample Frequency	Units	Data Product Number
PRT resistance at temperature T (R_t)	1 Hz	Ω	NEON.DOM.SITE.DP0.00002.001.01325.HOR.VER.000
Turbine Speed (S_T)	1 Hz	RPM	NEON.DOM.SITE.DP0.00002.001.01330.HOR.VER.000
Heater Status (H)	State Change	Binary	NEON.DOM.SITE.DP0.00002.001.01319.HOR.VER.000
2D Sonic Anemometer U component (*U*)	1 Hz	$m\ s^{-1}$	NEON.DOM.SITE.DP0.00001.001.01306.HOR.VER.000
2D Sonic Anemometer V component (*V*)	1 Hz	$m\ s^{-1}$	NEON.DOM.SITE.DP0.00001.001.01307.HOR.VER.000

3.3 Product Instances

Multiple SAATS will be deployed at tower sites. SAATS will be located on each boom arm below the top of the tower. A single SAAT will be deployed at aquatic sites. The AIS SAAT will be located on the aquatic met station 3m above ground level.

3.4 Temporal Resolution and Extent

One- and thirty-minute averages of temperature will be calculated to form L1 DPs.

3.5 Spatial Resolution and Extent

Each SAATS will represent the point at which it is placed on the tower infrastructure and aquatic met station. Ultimately, a temperature profile will be developed for each tower site from the array of

SAATSs on the tower (see AD[11] for detail on sensor placement for a specific core site, and AD[12] for description of the algorithms used for deriving this profile).

4 SCIENTIFIC CONTEXT

Temperature is one of the most fundamental physical measurements. It is a primary driving factor for countless physical, chemical, and biological processes. Temperature measurements will provide NEON with ancillary data for numerous other environmental measurements.

4.1 Theory of Measurement

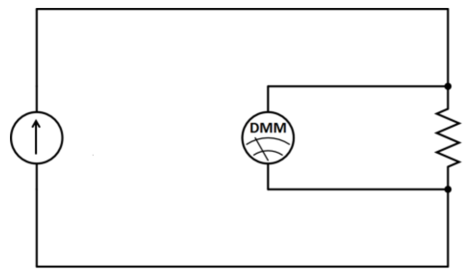

Figure 1. Four-wire measurement for PRT.

Ultimately, temperature is derived from a PRT. Changes in the PRT resistance due to temperature are determined using a four-wire measurement. The four-wire measurement was chosen due to its decreased dependence on cable length and resistors over the four-wire bridge method. Using a fixed current source the four-wire measurement detects a voltage drop across a resistor using a digital multi-meter (DMM) with high impedance, shown in Figure 1. The voltage drop across the PRT is used, in conjunction with known current source, to calculate the PRT resistance. This measurement technique accomplished by a DMM (i.e. GRAPE) will acquire resistance for NEON operated PRTs.

4.2 Theory of Algorithm

The PRT is one of the most widely used RTD because platinum has the best linear relationship for changes in resistance to temperature over the greatest temperature range (−200 to 650 °C). Normally, when evaluating temperatures over the entire range of the PRT, the relationship between temperature and resistance for a PRT is expressed by two equations due a divergence from linearity. However, NEON is concerned with only a fraction of the PRT's functional range. Thus, within NEON's desired temperature range the relationship between temperature and resistance is simplified and temperature as a function of resistance is expressed by a single equation (AD[10]):

$$T_i = C_2 * R_{T_i}^2 + C_1 * R_{T_i} + C_0 \tag{1}$$

Where:

T_i = Individual (1 Hz) Temperature (°C)
C_0 = Calibration coefficients provided by CVAL (°C)
C_1 = Calibration coefficients provided by CVAL (°C/Ω)

C_2 = Calibration coefficients provided by CVAL (°C/Ω^2)
R_{T_i} = Individual (1 Hz) resistance at temperature T (Ω)

Once PRT resistance has been converted to temperature one-minute $(\bar{T}_1)$ and thirty-minute $(\bar{T}_{30})$ averages of temperature will be determined according to Eq. (2) and (3) to create the file sat_datapub_NEONDOC002874.txt. However, individual calibrated measurements, i.e. 1 Hz temperature, will be made available upon request.

$$\bar{T}_1 = \frac{1}{n}\sum_{i=1}^{n} T_i \qquad (2)$$

where, for each 1-minute average, n is the number of measurements during the averaging period and T_i is a 1-Hz temperature measurement taken during the 60-second averaging period [0, 60). For a 1-minute average, n = 60 if all data points are included.

Similarly,

$$\bar{T}_{30} = \frac{1}{n}\sum_{i=1}^{n} T_i \qquad (3)$$

where, for each 30-minute average, n is the number of measurements during the averaging period and T_i is a 1-Hz temperature measurement taken during the 1800-second averaging period [0, 1800).

Note: The beginning of the first averaging period in a series shall be the nearest whole minute less than or equal to the first timestamp in the series.

5 ALGORITHM IMPLEMENTATION

Data flow for signal processing of L1 DPs will be treated in the following order.

1. 1 Hz resistance data will be converted to temperature, T_i, according to Eq. (1) using PRT calibration coefficients provided by CVAL.
2. QA/QC Plausibility tests will be applied to the data stream in accordance with AD[06], details are provided below.
3. Signal de-spiking will be applied to the data stream in accordance with AD[07].
4. One- and thirty-minute temperature averages will be calculated using Eq. (2) and (3).
5. Descriptive statistics, i.e. minimum, maximum, and variance, will be determined for both one- and thirty-minute averages.
6. QA/QC consistency tests will be applied to one- and thirty-minute averages in accordance with AD[05].

7. Quality metrics, quality flags, and the final quality flag will be produced for one- and thirty-minute averages according to AD[16].

QA/QC Procedure:

1. **Plausibility Tests** AD[06] – All plausibility tests will be determined for the SAAT. Test parameters will be provided by FIU and maintained in the CI data store. All plausibility tests will be applied to the sensor's converted L0 DPs and associated quality flags (QFs) will be generated for each test.

2. **Sensor Flags** – Sensor flags (i.e., flow rate and heater) are derived from L0 data products identified in the C^3 document (AD[09]). Any L0 DP (i.e., 1 Hz data) that has a heater flag applied will not be used to compute L1 DPs. Quality reports will be created for these flags as described in AD[16].

   a. Heater:

$$QF\_H = \begin{cases} 1 \;\; if \;\; t_i < t < t_i + (1.5 * Z) \\ 0 \;\; otherwise \end{cases}$$

Where:

t = Current timestamp
t_i = Timestamp that the heater last turned on, i.e. state change of *H* (NEON.DXX.XXX.DP0.00002.001.004.001.XXX.001) in AD[09]
Z = Amount of time that the heater stays on for one cycle AD[09]

The heater flag tests whether the heater is on, or was on during the preceding time interval. Data will continue to be flagged after the heater shuts off for half of the time the heater was operating in order to allow for heat to dissipate around the aspirated shield.

   b. Flow Rate:

The flow rate quality flag (QF_F) indicates whether the sensor is adequately aspirated. If the sensor is not adequately aspirated the quality flag will be set high, i.e. QF_F = 1, and QF_F = 0 otherwise. To determine whether sufficient aspiration is present QF_F incorporates the turbine speed, i.e., S_T, as well as the 1 Hz 2D wind speed measurement from the corresponding tower level. 2D wind speed is needed to account for bias in the turbine measurement when wind speeds are > 12 m/s. Thus, 1 Hz horizontal wind speed will need to be determined from data products NEON.DXX.XXX.DP0.00001.001.001.001.XXX.001 and

NEON.DXX.XXX.DP0.00001.001.002.001.XXX.001 according to Eq. (3) in AD[17]. Once the corresponding wind speed, i.e., W_s, has been determined the QF_F will be set accordingly:

$$QF\_F = \begin{cases} 1 \ \ if \ \ \frac{1}{n}\sum_{i=1}^{n} S_{T_i} < 650 \ RPM \ and \ W_s < 12 \text{ m/s} \\ \\ 0 \ \ otherwise \end{cases}$$

Where, n is the number of observations captured in a 30 second interval. It is necessary to average the turbine speed over a thirty second period due to the resolution of the sensor, which is digitized to intervals of 30 RPM. W_s is determined as the 1Hz wind speed that corresponds to the last 1Hz turbine measurement in a 30 second average, where the one second period is defined as ϵ [0.000000, 1.000000) seconds. For a given flow rate flag, its status will be applied to the corresponding 30 second interval of 1 Hz temperature measurements that were captured during its computation, where a 30 second period is defined as ϵ [0.000000, 30.000000) seconds.

3. **Signal De-spiking**– Time segments and threshold values for the automated de-spiking QA/QC routine will be specified by FIU and maintained in the CI data store. QFs from the de-spiking analysis will be applied according to AD[07].

4. **Consistency Analysis** – A QF for data consistency (QF_V) will be applied according to the consistency analysis outlined in AD[05], and a pass/fail flag will be generated to reflect this activity. To evaluate temperature for consistency at terrestrial sites, L1 temperature from a given SAATS will first be compared to the SAATS above it on the tower infrastructure. If a difference between the two temperature measurements is less than the defined limits, provided by FIU and maintained in the CI data store, then the sensor will have passed the consistency analysis. Alternatively, a temperature difference between the SAATS outside the defined limits will result in a failed test. A failed test from the above sensor will result in the SAATS being compared to the SAATS below it; if this too results in a failed test then the SAATS will have failed the consistency test and be flagged as such. If the SAATS fails the first test but passes the second then it will have passed the consistency test. This structure helps to ensure that non-functional sensors (e.g., sensors that are faulty or down for service) do not bias the test, since a resulting failed test will allow the sensor to be compared to the one below it. Accordingly, the SAATS on the bottom of the tower will only be compared to the SAATS above it and the uppermost SAATS will first be compared to the TRAATS and then to the SAATS below it. To evaluate temperature for consistency at aquatic sites, L1 temperature from the SAAT will be

compared to the RH temperature reported from the HMP155 sensor on the aquatic met station. If the difference between the two temperature measurements is less than the defined limits, provided by AQU and maintained in the CI data store, then the sensors will have passed the consistency analysis. L1 DPs that fail the consistency analysis will continue to be reported, but will have an associated failed QF that will be include in the QA/QC summary.

5. **Quality Flags (QFs) and Quality Metrics (QMs)** AD[16] – If a datum has failed one of the following tests it will not be used to create a L1 DP, ***range, persistence, step, heater,*** *and* ***flow***. α and β QFs and QMs will be determined for all of the external flags, Table 5-1. In addition, L1 DPs will have a QA/QC report and quality metrics associated with each flag listed in Table 5-1 as well as a final quality flag, as detailed in AD[16]. Ancillary information needed for the algorithm and other information maintained in the CI data store is shown in Table 5-2.

Table 5-1: Flags associated with SAATS measurements.

Tests
Range
Persistence
Step
Null
Gap
Signal Despiking
Consistency
Sensor Test AD[09]
Alpha
Beta
Final quality flag

Table 5-2: Information maintained in the CI data store for SAATS.

Tests/Values	CI Data Store Contents
Range	Minimum and maximum values
Persistence	Window size, threshold values and maximum time length
Step	Threshold values
Null	Test limit
Gap	Test limit

Signal Despiking	Time segments and threshold values
Calibration	CVAL sensor specific calibration coefficients
Uncertainty	AD[15]
Sensor Test	heater and flow thresholds
Consistency Analysis	Test limits
Final Quality Flag	AD[16]

6 UNCERTAINTY

Uncertainty of measurement is inevitable; therefore, measurements should be accompanied by a statement of their uncertainty for completeness (JCGM 2008; Taylor 1997). To do so, it is imperative to identify all sources of measurement uncertainty related to the quantity being measured. Quantifying the uncertainty of TIS measurements will provide a measure of the reliability and applicability of individual measurements and TIS data products. This portion of the document serves to identify, evaluate, and quantify sources of uncertainty relating to individual, calibrated SAAT measurements as well as L1 mean SAAT data products. It is a reflection of the information described in AD[13], and is explicitly described for the SAAT assembly in the following sections.

6.1 Uncertainty of Temperature Measurements

Uncertainty of the SAAT assembly is discussed in this section. The section is broken down into two topics. The first informs the sources of *measurement* uncertainty, i.e., those associated with *individual temperature measurements*. The second details uncertainties associated with temporally averaged temperature data products. A diagram detailing the data flow and known sources of uncertainty are displayed in Figure 2.

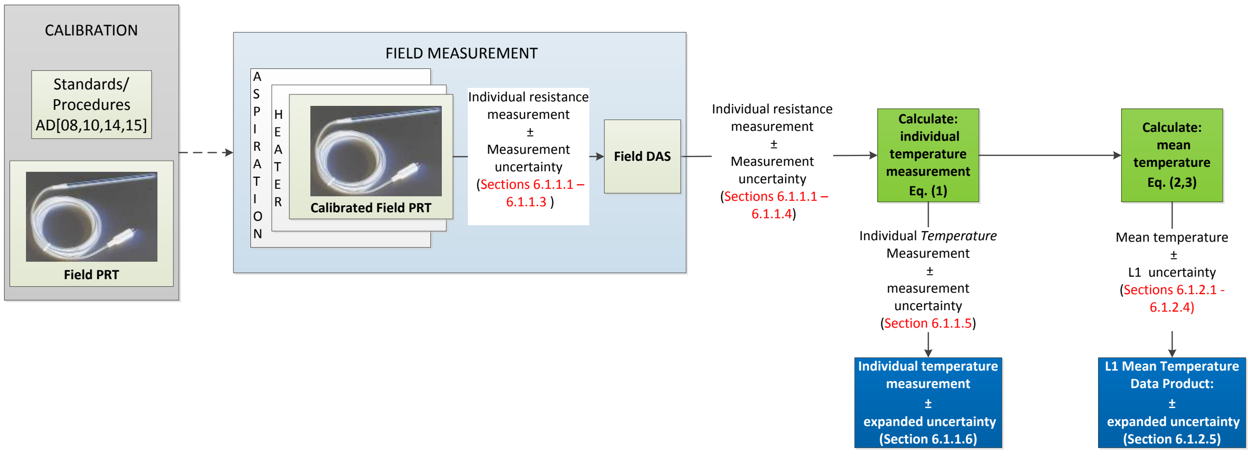

Figure 2: Displays the data flow and associated uncertainties of individual temperature measurements and L1 mean SAAT DPs. A detailed explanation of the PRT calibration procedures, please refer to AD[08,10,14].

6.1.1 Measurement Uncertainty

The following subsections present the uncertainties associated with *individual temperature observations*. It is important to note that the uncertainties presented in the following subsections are *measurement uncertainties*, that is, they reflect the uncertainty of an *individual* temperature measurement. These uncertainties should not be confused with those presented in Section 6.1.2. We urge the reader to refer to AD[13] for further details concerning the discrepancies between quantification of measurement uncertainties and L1 uncertainties.

NEON calculates measurement uncertainties according to recommendations of the Joint Committee for Guides in Metrology (JCGM) 2008. In essence, if a measurand *y* is a function of *n* input quantities

$x_i\ (i = 1, \ldots, n),\ i.e., y = f(x_1, x_2, \ldots, x_n)$, the combined measurement uncertainty of *y*, assuming the inputs are independent, can be calculated as follows:

$$u_c(y) = \left(\sum_{i=1}^{N} \left(\frac{\partial f}{\partial x_i} \right)^2 u^2(x_i) \right)^{\frac{1}{2}} \quad (4)$$

where

$\frac{\partial f}{\partial x_i}$ = partial derivative of *y* with respect to x_i

$u(x_i)$ = combined standard uncertainty of x_i.

Thus, the uncertainty of the measurand can be found be summing the input uncertainties in quadrature. For temperature measurements, the sources of uncertainty are depicted in Figure 2. The calculation of these input uncertainties is discussed below.

6.1.1.1 Calibration

Uncertainties associated with the PRT calibration process propagate into a standard, combined measurement uncertainty. This combined uncertainty, u_{A1}, represents i) the repeatability and reproducibility of the sensor and the lab DAS and ii) uncertainty of the calibration procedures and coefficients including uncertainty in the standard (truth) (refer to Eq. (1)). It is a constant value that will be provided by CVAL (AD[15]), stored in the CI data store, and applied to all *individual temperature measurements* (that is, it does not vary with any specific sensor, DAS component, location, etc.). A detailed summary of the calibration procedures and corresponding uncertainty estimates can be found in AD[08,10,14].

6.1.1.2 Heater

Throughout Observatory, the exteriors of aspirated shields are partially wrapped in heating material. This material will be turned on during times when ice buildup causes a potential threat to the aspiration within the shield (refer to AD[09] for specifics). When the heater is on, it is hypothesized that a portion of the thermal energy will conduct through the aluminum shield, thus altering the internal temperature of the shield and cause measurement bias.

At this time the extent to which the heater will affect the measurement uncertainty is unclear. Because of this, any measurements recorded during times of heating, and for a specified time after the heater is turned off (refer to Section 5), will be flagged. This is an example of an uncertainty that can be identified but cannot be quantified at this time.

6.1.1.3 Aspiration

The WMO (2006) argues that aspirated shields, i.e., those that utilize fan-forced air, result in more accurate temperature measurements than naturally ventilated (passive) shields. However, this is assuming that aspiration within the shield is of a magnitude that minimizes the effects of incoming solar radiation. Aspirated shields offer minimal natural ventilation given their design (i.e., non-perforated sides hinder natural ventilation), and large temperature errors may be possible if aspiration slows or ceases.

Met One (1997) states that their 076B aspirated shield reduces temperature biases to $< 0.05\ °F$ $(0.028\ ℃)$ at 1120 W m^{-2} of incoming solar radiation; this is also assuming that aspiration within the shield is approximately $500\ F^3\ min^{-1}(0.236\ m^3\ s^{-1})$. Unfortunately, the latter is the only uncertainty metric that Met One (1997) supplies. The company does not supply uncertainty estimates as functions of varying magnitudes of insolation or aspiration. Thus, their statement can be thought of as a worst case uncertainty (in regards to a large insolation rate), *applicable only when the aspiration within the shield is maintained at ~$0.236\ m^3\ s^{-1}$.* It is unclear how large these temperature biases could be if the aspiration within the shield slows or ceases.

Studies involving both passively ventilated and fan-forced (aspirated) shields show that temperature errors are a function of both ventilation/aspiration and insolation (e.g., Brock *et al*. 1995; Lin *et al*. 2000; Tarara and Hoheisel 2007). Brock *et al*. (1995) noted that when natural ventilation fell below 2 m s^{-1} and insolation rose above 700 W m^2, temperature errors were > 2°C for multi-plate, passively ventilated shields. Tarara and Hoheisel (2007) found that non-perforated, tube-shaped, aspirated shields were prone to larger temperature errors than naturally ventilated shields when aspiration ≤ 1 m s^{-1} and insolation ≥ 600 W m^{-2}. On the contrary, the authors also showed that temperature errors were *negligible* when ventilation/aspiration was ≤ 1 m s^{-1} and insolation < 200 W m^{-2}, for any type of shield, whether passively ventilated or aspirated.

Given the findings of the previous researchers it seems plausible that large temperature may be possible if aspiration of Met One's 076B shield completely ceases while insolation is > 200 W m^2. As stated previously, the magnitudes of these errors are currently unknown. In the future it may be possible to derive sufficient aspirations, i.e., those that minimize temperature bias, as a function of insolation. For instance, following Tarara and Hoheisel (2007), aspiration ≤ 1 m s^{-1} may be acceptable if insolation is < 200 W m^2, however, it also may be possible that aspiration should be ≥ 4.0 m s^{-1} to minimize temperature biases during periods when insolation is ≥ 800 W m^2.

As a safe approach we assume that temperatures measured when aspiration is << $0.236\ m^3\ s^{-1}$ are accompanied by an unquantifiable systematic uncertainty. During these instances data will be flagged and will not be used to calculate L1 DPs. At current date, NEON will not correct for the temperature bias described by Met One (1997). We encourage the end-user to use scientific judgment when applying this 0.028 °C temperature bias, and caution that this bias may be unrepresentative of actual biases over a range of incoming solar radiation and aspiration rates.

6.1.1.4 Field DAS

The uncertainty introduced by the Field DAS (FDAS) through the resistance reading is:

$$u_{FDAS}(R_{T_i}) = (u_{R1} * R_{T_i}) + O_R \qquad (5)$$

Where:

$u_{FDAS}(R_{T_i})$	= standard uncertainty of the resistance measurement introduced by the Field DAS (Ω)
R_{T_i}	= *individual,* raw, resistance measurement (Ω)
u_{R1}	= combined, relative Field DAS uncertainty for resistance measurements provided by CVAL (unitless)
O_R	= offset imposed by the FDAS for resistance readings, provided by CVAL (Ω)

The partial derivative of a temperature measurement with respect to the resistance reading is:

$$\frac{\partial T_i}{\partial R_{T_i}} = (2 * C_2 * R_{T_i}) + C_1; \tag{6}$$

therefore, the uncertainty of a temperature measurement due to the FDAS is:

$$u_{FDAS_{R_T}}(T_i) = \left|\frac{\partial T_i}{\partial R_{T_i}}\right| u_{FDAS}(R_{T_i}) \tag{7}$$

where:

$\frac{\partial T_i}{\partial R_{T_i}}$	= partial derivative of Eq. (1) with respect to R_{T_i} (°C/Ω)
C_2	= calibration coefficient provided by CVAL (°C/Ω^2)
C_1	= calibration coefficient provided by CVAL (°C/Ω)
$u_{FDAS_{R_T}}(T_i)$	= standard uncertainty of temperature introduced by the Field DAS through the resistance measurement (°C)

6.1.1.5 Combined Measurement Uncertainty

The combined, standard, measurement uncertainty for an individual temperature measurement, $u_c(T_i)$, is given in units of °C and computed by summing the individual uncertainties in quadrature (Eq. (4)):

$$u_c(T_i) = \left(u_{A1}^2 + u_{FDAS_{R_T}}^2(T_i)\right)^{\frac{1}{2}} \tag{8}$$

6.1.1.6 Expanded Measurement Uncertainty

The expanded measurement uncertainty is calculated as:

$$U_{95}(T_i) = k_{95} \ * u_c(T_i) \tag{9}$$

Where:

$U_{95}(T_i)$ = expanded measurement uncertainty at 95% confidence (°C)

k_{95} = 2; coverage factor for 95% confidence (unitless)

6.1.2 Uncertainty of L1 Mean Temperature Data Product

The following subsections discuss uncertainties associated with L1 mean temperature data products. As stated previously, it is important to note the differences between the *measurement uncertainties* presented in Section 6.1.1 and the uncertainties presented in the following subsections. The uncertainties presented in the following subsections reflect the uncertainty of a time-averaged mean value, that is, they reflect the uncertainty of a distribution of measurements collected under non-controlled conditions (i.e., those found in the field), as well as any uncertainties, in the form of *Truth* and *Trueness*, related to the accuracy of the field assembly.

6.1.2.1 Repeatability (natural variation)

To determine the validity of the L1 mean temperature DP, its uncertainty must be calculated. The distribution of the individual measurements is used as a metric to quantify this uncertainty. Specifically, the *estimated standard error of the mean (natural variation)* is computed. This value reflects the repeatability of temperature measurements for the specified time period:

$$u_{NAT}(\bar{T}) = \frac{s(T_i)}{\sqrt{n}} \quad [°C] \tag{10}$$

where $s(T_i)$ is the experimental standard deviation of the temperature observations during the averaging period, and n is the number of observations made over the same time period.

6.1.2.2 Calibration

The uncertainty detailed here is similar to that described in Section 6.1.1.1. However, the relevant uncertainty for the mean DPs, u_{A3}, does not consider i) individual sensor repeatability, or ii) the variation of sensors' responses over a population of sensors (reproducibility). This component of uncertainty estimates the uncertainty due to the accuracy of the instrumentation in the form of *Truth* and *Trueness*, a quantity which is not captured by the standard error of the mean. It is a constant value that will be provided by CVAL (AD [15]) and stored in the CI data store. Please refer to AD[13] for further justification regarding evaluation and quantification of this combined uncertainty.

6.1.2.3 Field DAS

Since the L1 mean temperature DP is a function of the individual temperature measurements, any measurement bias introduced by the Field DAS will be reflected in the L1 mean data product. Here, the raw measurement(s) that maximize the combined uncertainty of an individual measurement (Eq. (8)) is used in the calculation of the L1 mean DP uncertainty. Uncertainty components due to random effects, whether a function of the environment or the measurement assembly, are quantified via the natural variation of the mean (see Section 6.1.2.1). For more information regarding the justification of this approach, please see AD[13].

The accuracy of the Field DAS in the form of *Truth* and *Trueness* propagates through to the uncertainty of the mean DP similarly to how the Field DAS uncertainty associated with a raw resistance propagates through to the uncertainty of the measurement attributable to the Field DAS (Eqs.(5)-(7)).

$$u_{FDAS(TT)}\left(R_{T\,MAX}\right) = \left(u_{R3} * R_{T\,MAX}\right) + O_R \tag{11}$$

Where, the subscript "MAX" represents the index, i, where the *maximum*, combined, standard, measurement uncertainty of SAAT is observed over a set (averaging period) of observations. Mathematically, this can be defined as:

$$MAX = \{i: u_c(T_i) = \max[u_c(T_1), \dots, u_c(T_n)]\}. \tag{12}$$

Also,

$u_{FDAS(TT)}\left(R_{T_{MAX}}\right)$	= Field DAS *Truth* and *Trueness* uncertainty of $R_{T_{MAX}}$(Ω)
$R_{T\,MAX}$	= individual, raw, resistance measurement observed at MAX index (Ω)
u_{R3}	= relative, combined, Field DAS *Truth* and *Trueness* for resistance measurements, provided by CVAL (unitless)
O_R	= offset imposed by the FDAS for resistance measurements, provided by CVAL (Ω)

Thus, analogous to Eq. (7),

$$u_{FDAS(TT)}(\bar{T}) = \left|\frac{\partial T_i}{\partial R_{T_i}}\right|_{R_{T\,MAX}} u_{FDAS(TT)}\left(R_{T\,MAX}\right), \tag{13}$$

where:

$\left\|\frac{\partial T_i}{\partial R_{T_i}}\right\|_{R_{T\,MAX}}$	= partial derivative of T_i with respect to R_{T_i} (Eq. (6)) evaluated at $R_{T\,MAX}$ (°C/Ω)
$u_{FDAS(TT)}(\bar{T})$	= *Truth* and *Trueness* uncertainty of the mean DP introduced by the Field DAS (°C)

6.1.2.4 Combined Uncertainty

The combined uncertainty for our L1 mean temperature data product, $u_c(\bar{T})$, is given in units of °C and computed by summing the uncertainties from Sections 6.1.2.1 through 6.1.2.3 in quadrature:

$$u_c(\bar{T}) = \left(u_{NAT}^2(\bar{T}) + u_{A3}^2 + u_{FDAS(TT)}^2(\bar{T})\right)^{\frac{1}{2}} \quad (14)$$

6.1.2.5 Expanded Uncertainty

The expanded uncertainty is calculated as:

$$U_{95}(\bar{T}) = k_{95} * u_c(\bar{T}) \quad (15)$$

Where:

$U_{95}(\bar{T})$	= expanded L1 mean data product uncertainty at 95% confidence (°C)
k_{95}	= 2; coverage factor for 95% confidence (unitless)

6.2 Uncertainty Budget

The uncertainty budget is a visual aid detailing i) quantifiable sources of uncertainty, ii) means by which they are derived, and iii) the order of their propagation. Uncertainty values denoted in this budget are either derived within this document or are provided by other NEON teams (e.g., CVAL), and stored in the CI data store.

Table 6-1: Uncertainty budget for an individual temperature measurement. Shaded rows denote the order of uncertainty propagation (from lightest to darkest).

Source of measurement uncertainty	**Measurement uncertainty component $u(x_i)$**	**Measurement uncertainty value**	$\frac{\partial f}{\partial x_i}$	$u_{x_i}(Y) \equiv \left\|\frac{\partial f}{\partial x_i}\right\| u(x_i)$ **[°C]**
\1 Hz temp.	$u_c(T_i)$	Eq. (8) [°C]	n/a	n/a
Sensor/calibration	u_{A1}	AD[15] [°C]	1	u_{A1}
FDAS	$u_{FDAS}(R_{T_i})$	Eq. (5) [Ω]	Eq. (6)	Eq. (7)

Table 6-2: Uncertainty budget for L1 mean temperature measurements. Shaded rows denote the order of uncertainty propagation (from lightest to darkest).

Source of uncertainty	**Uncertainty component $u(x_i)$**	**Uncertainty value**	$\frac{\partial f}{\partial x_i}$	$u_{x_i}(Y) \equiv \left\|\frac{\partial f}{\partial x_i}\right\| u(x_i)$ **[°C]**
L1 mean temp	$u_c(\bar{T})$	Eq. (14) [°C]	n/a	n/a
Natural variation	$u_{NAT}(\bar{T})$	Eq. (10) [°C]	1	Eq. (10)
Sensor(TT)	u_{A3}	AD[15] [°C]	1	u_{A3}
FDAS(TT)	$u_{FDAS(TT)}(R_{T\,MAX})$	Eq. (11) [Ω]	Eq. (6)	Eq. (13)

7 FUTURE PLANS AND MODIFICATIONS

Future system flags may be incorporated into the data stream. Additionally, individual calibrated and QA/QCd measurements with their respective uncertainties may become a common data output in the future.

Details concerning the evaluation and quantification of Sensor and Field DAS drift will be added to the uncertainty section

8 BIBLIOGRAPHY

Brock, F. V., S. J. Richardson, and S.R. Semmer, (1995) Passive multi-plate solar shields. 9th Symp. Meteor. Obs. And Inst., pp 179-183.

Joint Committee for Guides in Metrology (JCGM) (2008) Evaluation of measurement data – Guide to the expression of uncertainty in measurement. pp. 120.

JCGM (2012) International vocabulary of metrology – Basic and general concepts and associated terms (VIM). 3rd Edition. pp. 92

Lin, X., K. G. Hubbard, and G. E. Meyer, (2000) Airflow Characteristics of Commonly Used Temperature Radiation Shields, Journal of Atmospheric and Oceanic Technology, **18**, pp. 329–339.

Met One Instruments, Inc. (1997) Fan Aspirated Radiation Shield: Specification Sheet. Rev. 076B, pp. 2.

Richardson, S. J., F.V. Brock, S.R. Semmer, C. Jirak, (1999) Minimizing errors Associated with Multi-plate Radiation Shields, Journal of Atmos. And Ocean. Tech., **16**, pp 1862-1872.

Tarara J. M., and Hoheisel G. (2007) Low-cost shielding to minimize radiation errors of temperature sensors in the field. *HortScience*, **42**, 1372-1379

Taylor, J. R. (1997) An Introduction to Error Analysis: The Study of Uncertainties in Physical Measurements. University Science Books, Mill Valley, California. 2nd Ed. pp. 327.

World Meteorological Organization (WMO) (2006) Guide to meteorological instruments and methods of observation: Measurement of Temperature. WMO-No. 8.